Hot flow anomaly observed at Jupiter's bow shock

P. W. Valek, M. F. Thomsen, F. Allegrini, F. Bagenal, S. Bolton, J. Connerney, R. W. Ebert, R. Gladstone, W. S. Kurth, S. Levin, et al.

AGU PUBLICATIONS

Geophysical Research Letters

RESEARCH LETTER
10.1002/2017GL073175

Special Section:
Early Results: Juno at Jupiter

Hot flow anomaly observed at Jupiter's bow shock

P. W. Valek[1,2], M. F. Thomsen[3], F. Allegrini[1,2], F. Bagenal[4], S. Bolton[1], J. Connerney[5], R. W. Ebert[1], R. Gladstone[1,2], W. S. Kurth[6], S. Levin[7], P. Louarn[8], B. Mauk[9], D. J. McComas[1,10,11], C. Pollock[12], M. Reno[1,13], J. R. Szalay[1], S. Weidner[11], and R. J. Wilson[4]

[1]Space Science and Engineering Division, Southwest Research Institute, San Antonio, Texas, USA, [2]Department of Physics and Astronomy, University of Texas at San Antonio, San Antonio, Texas, USA, [3]Planetary Science Institute, Tucson, Arizona, USA, [4]Laboratory for Atmospheric and Space Physics, University of Colorado Boulder, Boulder, Colorado, USA, [5]Goddard Space Flight Center, Greenbelt, Maryland, USA, [6]Department of Physics and Astronomy, University of Iowa, Iowa City, Iowa, USA, [7]Jet Propulsion Laboratory, Pasadena, California, USA, [8]Université de Toulouse, IRAP, CNRS, UPS, Toulouse, France, [9]The Johns Hopkins University Applied Physics Laboratory, Laurel, Maryland, USA, [10]Department of Astrophysical Sciences, Princeton University, Princeton, New Jersey, USA, [11]Office of the Vice President for the Princeton Plasma Physics Laboratory, Princeton University, Princeton, New Jersey, USA, [12]Denali Scientific, Healy, Alaska, USA, [13]Austin Mission Consulting, Austin, Texas, USA

Key Points:
- Observations from Juno of the first Hot Flow Anomaly detected at Jupiter's bow shock
- Size of Jovian Hot Flow Anomaly is orders of magnitude larger than those seen at other planets
- Size of Hot Flow Anomalies scale with the size of the bow shock of the planet

Correspondence to:
P. W. Valek,
pvalek@swri.edu

Citation:
Valek, P. W., et al. (2017), Hot flow anomaly observed at Jupiter's bow shock, *Geophys. Res. Lett.*, *44*, 8107–8112, doi:10.1002/2017GL073175.

Received 20 FEB 2017
Accepted 18 APR 2017
Published online 18 AUG 2017

Abstract A Hot Flow Anomaly (HFA) is created when an interplanetary current sheet interacts with a planetary bow shock. Previous studies have reported observing HFAs at Earth, Mercury, Venus, Mars, and Saturn. During Juno's approach to Jupiter, a number of its instruments operated in the solar wind. Prior to crossing into Jupiter's magnetosphere, Juno observed an HFA at Jupiter for the first time. This Jovian HFA shares most of the characteristics of HFAs seen at other planets. The notable exception is that the Jovian HFA is significantly larger than any HFA seen before. With an apparent size greater than 2×10^6 km the Jovian HFA is orders of magnitude larger than those seen at the other planets. By comparing the size of the HFAs at the other planets with the Jovian HFA, we conclude that HFAs size scales with the size of planetary bow shocks that the interplanetary current sheet interacts with.

1. Introduction

A Hot Flow Anomaly (HFA) is created when an interplanetary current sheet interacts with a planetary bow shock [*Schwartz*, 1995; *Schwartz et al.*, 2000]. The inward pointing motional electric field deflects and heats ions reflected from the bow shock. HFAs were first observed by AMPTE [*Schwartz et al.*, 1985] and by ISEE [*Thomsen et al.*, 1986] near the Earth's bow shock.

Key features of an HFA—as listed by *Schwartz et al.* [2000] based on observation at Earth's bow shock—are (1) a hot central region; (2) lower velocity than the bulk solar wind and strong deflection away from the Earth; (3) noisy interior magnetic field, with periods of depressed and enhanced B field; (4) compressed edge regions flanking the central region on one or both sides; (5) presence of an interplanetary current sheet as evidenced by different interplanetary magnetic field direction before and after the HFA; (6) proximity to the bow shock; and (7) a three-dimensional structure inferred from the shock normal. An eighth feature listed by *Schwartz et al.* [2000, item 4] was that the durations of these HFA lasted minutes, implying scale sizes of a few Earth radii.

HFAs appear to be a common phenomenon occurring in foreshocks of planets. HFAs have not only been observed at Earth but also at Mercury [*Uritsky et al.*, 2014], Venus [*Collinson et al.*, 2012], Mars [*Øieroset et al.*, 2001; *Collinson et al.*, 2015], and Saturn [*Masters et al.*, 2009]. The key features of the HFA are seen at the different foreshock regions, but typical size of the HFA does vary for the different planets [*Uritsky et al.*, 2014, and references within].

Prior to the Juno mission, no observations of an HFA in the vicinity of Jupiter have been reported. In this paper, we show the first observations of an HFA at Jupiter made during the approach to the planet by the Juno spacecraft. The transient events in the magnetic and plasma observations are presented here. We also discuss how the size of the Jovian HFA compares to the HFAs seen at other planets.

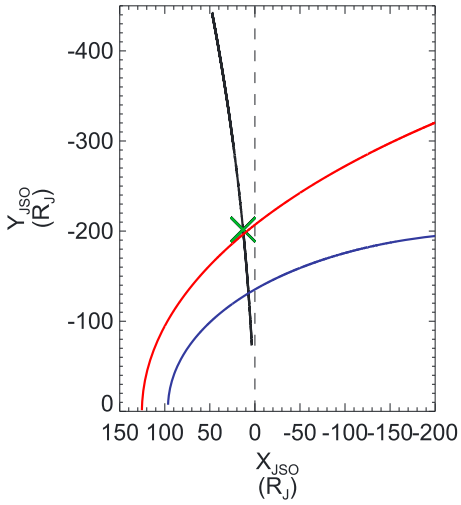

Figure 1. Juno approach trajectory. Plotted is the trajectory of the Juno spacecraft during the approach (black), the bow shock location (red), and the magnetopause location (blue) just prior to the HFA observations based on the model of *Joy et al.* [2002] and JADE solar wind observations. The location of the observed HFA is shown by the green cross.

2. Observations

The observations of the HFA come from the Jupiter Auroral Distributions Experiment (JADE) [*McComas et al.*, 2013] and the Juno Magnetic Field Investigation (MAG) [*Connerney et al.*, 2017b], both flown aboard the Juno spacecraft. MAG consists of a pair of fluxgate magnetometers and proximate star cameras for accurate mapping of the Jovian magnetic field. The magnetometers were designed to measure the wide range of magnetic field magnitudes, from interplanetary fields to the large fields observed near Jupiter [*Connerney et al.*, 2017a].

The JADE instrument was designed to measure the plasma environment in Jupiter's magnetosphere and auroral regions, using a suite of two electron sensors (JADE-E) and an ion sensor (JADE-I). It also makes measurements of the solar wind. JADE-I measures ions with an energy per charge between 10 eV/q and 46.5 keV/q with an energy resolution ($\Delta E/E$) of ~0.25 at 1 keV/q. The instantaneous field of view (FOV) of JADE-I is 270° × 8.5° and is aligned so that the full 4π view of the sky is covered once per spacecraft spin, nominally a 30 s spin period. During approach the Juno spin axis was pointing sunward, allowing JADE-I to continually observe the solar wind. JADE-E was not operated during the time period presented here.

For the data presented here, JADE-I was in its Low Rate Science (LRS) data collection mode. In this mode, the data are collapsed across its angular dimensions to reduce the required telemetry. The count rate, as opposed to the number of counts, is reported. The reported rates come from the eight anodes that view the 180° arc that runs from along the spacecraft positive spin axis to the negative spin axis, which looks outward from the spacecraft body.

The anode that looks along the spin axis has its data grouped into 22.5° × 120° (elevation × azimuth [spin]) bins. This is the anode which measures ions traveling in an antisunward direction. Since the solar wind is known to be cold [*Ebert et al.*, 2014] at these heliospheric distances, and therefore not fully fill the grouped angle bins, we assume that the solar wind fill 22.5° × 22.5° of the spin axis-aligned angle bins when we calculate the numerical moments. The moments in the solar wind therefore have significant uncertainties. The next anode has its data grouped in to 22.5° × 45° bins. The anodes that look radially outward have their data grouped into 22.5° × 24° bins. In the central region of the HFA the counts are observed primarily in the radially viewing anode.

The Juno mission approached Jupiter from the dawnside of the planet during mid-2016 [*Bagenal et al.*, 2014; *McComas et al.*, 2017]. During the approach phase of the mission, various instruments were operated to make observations in the solar wind at 5 AU. The trajectory of the spacecraft between 15 May and 29 June 2016 is shown in Figure 1. This is the period when observations of the solar wind and crossing into the Jovian magnetosphere are available from Juno [*Ebert et al.*, 2017; *McComas et al.*, 2017]. The nominal bow shock (magnetopause) is drawn in red (blue) as determined using the model of *Joy et al.* [2002] and a solar wind pressure of 0.029 ± 0.013 nPa as measured by JADE (Figure 2) prior to the HFA. On 15 June 2016 a HFA was observed by the Juno spacecraft. At the time of the HFA the Juno spacecraft was located at (13, −202, 39) R_J in the Jupiter-Sun-Orbit (JSO) coordinate system [*Bagenal et al.*, 2014].

Observations from JADE and MAG of the HFA are shown in Figure 2. During the period shown here, the JADE data have 600 s resolution and the magnetometer data have 1 s resolution. Moments presented in Figure 2 from JADE-I are calculated using two methods: (1) numerical integration based on the hot plasma approximation, which is appropriate for the hot central region (black curves) [*Paschmann and Daly*, 2000], and (2) forward modeling the observations with isotropic Maxwellians (blue curves). Since JADE was designed to measure magnetospheric rather than the solar wind plasmas, it has a broad energy resolution, $\Delta E/E$ ~ 0.25.

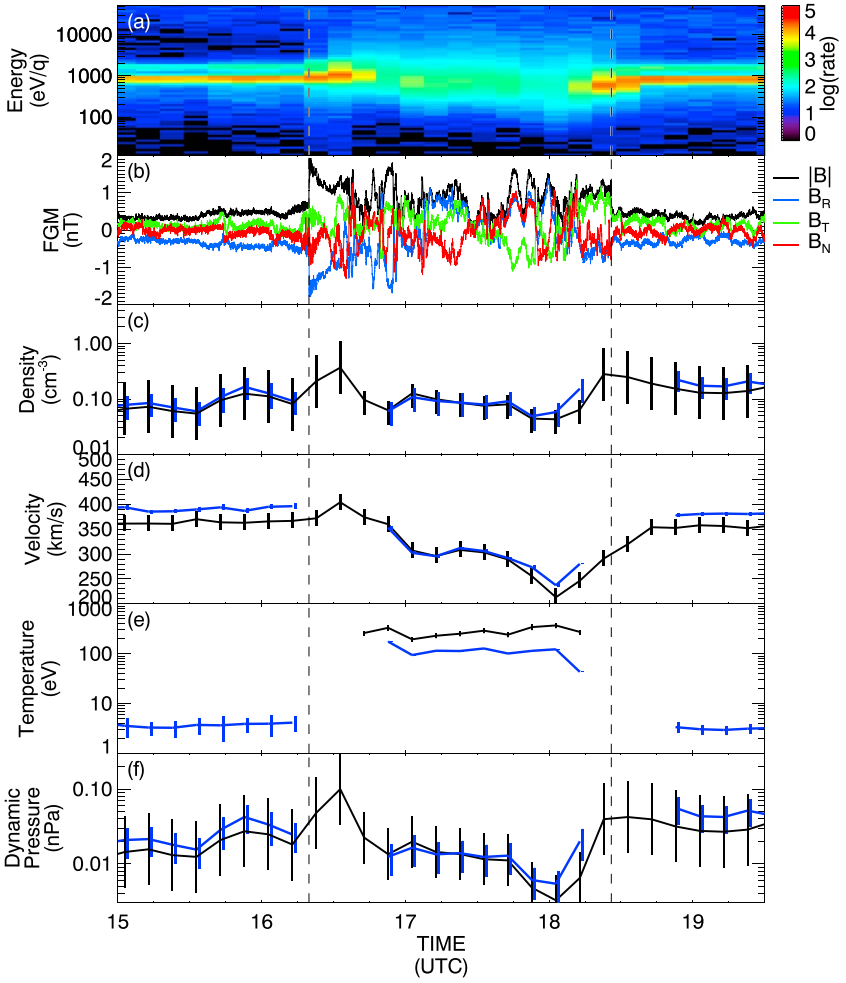

Figure 2. Summary of the HFA as observed by JADE and MAG on 15 June 2016. (a) The observed ion count rate from JADE. (b) The magnetic field in Spacecraft-Solar Equatorial (commonly Radial Tangent Normal (or RTN)) coordinates. The (c) Density, (d) Velocity, (e) Temperature, and (f) Pressure as observed by JADE. The black curves are determined from numerical moments, and the blue curves are from fits to a Maxwellian distribution. The vertical dashed lines indicate the boundary of the HFA as determined from the magnetic field data.

The JADE solar wind moments will generally have large uncertainties (~45% for density, less than 10% for velocity). Because of this wide energy resolution, the temperature calculated by the numerical moments in the solar wind is not shown. In the solar wind the forward model-derived moments (blue curves) are used. The forward modeling approach is necessary for JADE observations in the poorly resolved cold solar wind.

At the beginning and at the end of the interval shown in Figure 2, Juno was in the solar wind, as seen by the relatively cold ion distribution flowing at ~390 km/s. The interval between the vertical dashed lines is what we identify as the Hot Flow Anomaly. An energy-time ion spectrogram is shown in Figure 2a. Prior to the arrival of the HFA, two peaks are visible in the spectrogram for the solar wind protons and alphas. The ion energy spectra changes from a narrow distribution to a broad, hot distribution when the HFA arrives. The bulk velocity also changes direction in the HFA (Figure 3).

Qualitatively, the plasma and the field properties satisfy all of the key features of HFAs summarized by *Schwartz et al.* [2000]: (1) A hot central region (~1645–1815 UTC) with an ion temperature ~100 eV (10^6 K), which is comparable to HFAs observed at Earth and Saturn [*Thomsen et al.*, 1988; *Masters et al.*, 2009] (Figure 2e); (2) lower speed than the ambient solar wind (Figure 2d). The flow is also significantly deflected in the direction away from Jupiter (Figure 3); (3) a noisy magnetic field, with the field strength at times increasing over 1.5 nT and at other times dropping to near zero (Figure 2b); (4) a compressed edge as indicated by enhanced density (Figure 2c); (5) interplanetary current sheet as evidenced by the interplanetary

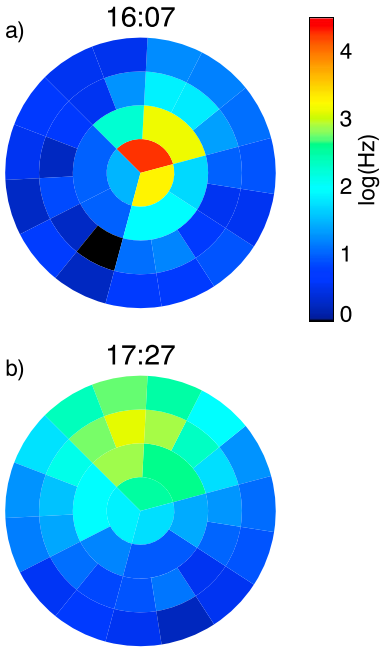

Figure 3. Incident direction of protons shown in a fish-eye projection. Antisunward flow is in the center of each panel, top of each panel is northward flow and flow toward Jupiter is toward the left. Each concentric ring maps to an anode and is 22.5° wide. While in the (a) solar wind the protons are traveling predominantly antisunward. In the (b) HFA the protons are observed ~45° from the antisunward direction.

magnetic field rotated by 37.4° across the HFA (Figure 2b); (6) proximity to the bow shock—location of HFA indicated by the cross in Figure 1 (see *McComas et al.* [2017] for a discussion of the bow shock crossing on DOY 176); and (7) three-dimensional structure inferred by the shock normal (Figure 2b). A summary of key observations is given in Table 1.

In addition to the list of feature above, another condition believed to be required for a HFA formation is that the ratio of the transit velocity of the discontinuity to the gyrovelocity of the reflected ion be less than 1. The normalized transit speed is calculated as in *Schwartz et al.* [2000] and is found to be 0.75 on the pre-HFA side on the discontinuity. The value of the pre-HFA magnetic field was determined as the average field over the interval between 16:10 and 16:20, and the post-HFA magnetic field as the average field over the interval between 18:26 and 18:36.

Compression regions are observed on both sides of the HFA. This is consistent with weakly shocked solar wind, indicative of rapid expansion of the hot central region of the HFA itself. Such flanking shocked regions have been noted at HFAs at other planets [e.g., *Fuselier et al.*, 1987]. The shocked plasma ahead of the HFA entry is actually flowing faster than the ambient solar wind, suggesting that it is a fast-forward shock propagating away from the expanding bubble located sunward of the spacecraft. At the trailing edge of the HFA, the shocked plasma is flowing more slowly than the ambient solar wind, consistent with a fast reverse shock propagating away from an expanding bubble located antisunward of the spacecraft. Thus, these shocked regions are consistent with an expanding HFA convecting antisunward across the spacecraft. Assuming that convection is at the ambient solar wind speed, as other analyses of HFAs have done, then HFA duration of 1.5 h (2.1 h), excluding (including) the shocked solar wind on each side, suggests that the HFA is ~2.1×10^6 (2.9×10^6) km across. This is 2 orders of magnitude larger than typical HFAs at Earth [*Facskó et al.*, 2009].

3. Discussion

We have presented here the first observations of a Hot Flow Anomaly in the vicinity of Jupiter. This HFA was observed by the Juno spacecraft as it approached Jupiter on the dawnside of the planet. The HFA occurrence rate at Earth has been estimated as three per day [*Schwartz et al.*, 2000]. The HFA occurrence rate at Saturn has been given as once per 15 days, however, that is considered a lower bound [*Masters et al.*, 2009]. The

Table 1. Properties of the HFA Observed by Juno

Parameter	Value	Remarks
IMF prior to current sheet (CS) (B_{pre})	[−0.48, 0.032, −0.19] nT	RTN[a] coordinates
IMF post-CS (B_{post})	[−0.33, −0.27, −0.048] nT	RTN[a] coordinates
CS normal ($N(B_{pre} \times B_{post})$)	[0.05, 0.04, −0.12]	
Change in IMF angle ($\theta(B_{pre} \cdot B_{post})$)	37.4°	
Electric Fields	Inward toward CS	
Solar wind velocity (V_{sw})	390 km/s	Average between 15 and 16 UTC
Size of HFA	2.1×10^6 km	1.5 h excluding shock
	(2.9×10^6 km)	(2.1 h including shock)
Normalized transit speed ($\lvert V_{tr}/V_g \rvert$)	0.75	Calculated on the pre-HFA side

[a]RTN is also known as Spacecraft-Solar Equatorial system.

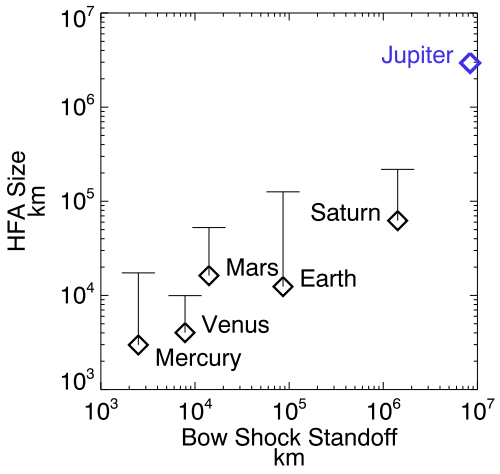

Figure 4. Comparison of typical sizes of HFA's for various planets. The typical HFA sizes are indicated by the diamonds, and the largest sizes are indicated by the bar. The typical and extreme HFA sizes and bow shock standoff distances for the planets other than Jupiter come from *Uritsky et al.* [2014].

one reported HFA observation at Jupiter does not allow us to make a reasonable estimate of the occurrence rate; however, the reason that no other HFAs have been seen at Jupiter may be that they are relatively rare.

The Jovian HFA has the characteristics of those seen at other planets, namely, a hot central region, a lower velocity than the bulk solar wind, a noisy magnetic field with periods of depressed and enhanced *B*, an interplanetary current sheet, proximity to the bow shock, and a three-dimensional structure. What makes the HFA observed at Jupiter different from those observed at other planets is the immense size of the structure. The size of the Jovian HFA is shown in relation to other planets in Figure 4. The data for the planets except Jupiter come from *Uritsky et al.* [2014, and references therein]. The Jovian HFA is orders of magnitude larger than HFAs typically seen at the other planets. From this single observation we cannot comment on the distribution of sizes at Jupiter, but it is clear that the HFA presented here is significantly larger than those seen at other planets.

Uritsky et al. [2014] observed that the size of HFAs from Mercury, Venus, Earth, Mars, and Saturn tended to increase with the size of the planetary bow shock. However, they did recognize an alternative explanation that the size of the HFAs could be related to the distance from the Sun, since larger distances from the Sun lead to larger ion scales describing an expanding solar wind [*Uritsky et al.*, 2011]. When compared in units of proton gyroradii (based on the statistical model by *Köhnlein* [1996]), the typical HFA sizes of the other planets are on the order of 200 gyroradii, ranging between ~140 and 290. However, the Jovian HFA presented here is ~15,000 gyroradii in size. Even the extreme HFAs are less than 3000 gyroradii, or over 5 times smaller than the Jovian HFA. Inclusion of the HFA observed at Jupiter suggests that it not the distance from the Sun but rather the bow shock size that is important for the size of the HFAs.

This suggests that an HFA continues to form along the interplanetary current sheet as it sweeps along the bow shock under conditions geometrically favorable to produce back streaming ions. These conditions are determined by the shock normal [e.g., *Burgess*, 1989; *Thomas et al.*, 1991, *Schwartz et al.*, 2000], which varies along the shock in a self-similar manner, so the region with the suitable conditions should scale with the size of the bow shock observed. For a larger bow shock, the current sheet would then be in contact with the region where the interplanetary current sheet/bow shock interaction is favorable for formation of an HFA for a longer time. This longer interaction would allow more time for ions to be channeled into the current sheet and hence produce a larger HFA.

Acknowledgments
This work was supported as a part of the work on NASA's Juno mission. We thank the many individuals who have made the Juno mission such a success. The JNO-J/SW-JAD-3-CALIBRATED-V1.0 and JNO-SS-3-FGM-CALIBRATED-V1.0 data sets were obtained from the Planetary Data System (PDS) at http://pds.nasa.gov/.

References

Bagenal, F., et al. (2014), Magnetospheric science objectives of the Juno mission, *Space Sci. Rev.*, 1–69, doi:10.1007/s11214-014-0036-8.
Burgess, D. (1989), On the effect of a tangential discontinuity on ions specularly reflected at an oblique shock, *J. Geophys. Res.*, *94*(A1), 472–478, doi:10.1029/JA094iA01p00472.
Collinson, G., et al. (2015), A hot flow anomaly at Mars, *Geophys. Res. Lett.*, *42*, 9121–9127, doi:10.1002/2015GL065079.
Collinson, G. A., et al. (2012), Hot flow anomalies at Venus, *J. Geophys. Res.*, *117*, a04204, doi:10.1029/2011JA017277.
Connerney, J. E. P., et al. (2017a), Jupiter's magnetosphere and aurorae observed by the Juno spacecraft during its first polar orbits, *Science*, doi:10.1126/science.aam5928.
Connerney, J. E. P., et al. (2017b), The Juno magnetic field investigation, *Space Sci. Rev.*, doi:10.1007/s11214-017-0334-z, in press.
Ebert, R. W., F. Bagenal, D. J. McComas, and C. M. Fowler (2014), A survey of solar wind conditions at 5 AU: A tool for interpreting solar wind-magnetosphere interactions at Jupiter, *Front. Astronomy Space Sci.*, *1*(4), doi:10.3389/fspas.2014.00004.
Ebert, R. W., et al. (2017), Accelerated flows at Jupiter's magnetopause: Evidence of magnetic reconnection along the dawn flank, *Geophys. Res. Lett.*, *44*, 4401–4409, doi:10.1002/2016GL072187.
Facskó, G., Z. Németh, G. Erdős, A. Kis, and I. Dandouras (2009), A global study of hot flow anomalies using cluster multi-spacecraft measurements, *Ann. Geophys.*, *27*(5), 2057–2076, doi:10.5194/angeo-27-2057-2009.

Fuselier, S. A., M. F. Thomsen, J. T. Gosling, S. J. Bame, C. T. Russell, and M. M. Mellott (1987), Fast shocks at the edges of hot diamagnetic cavities upstream from the Earth's bow shock, *J. Geophys. Res.*, *92*(A4), 3187–3194, doi:10.1029/JA092iA04p03187.

Øieroset, M., D. L. Mitchell, T. D. Phan, R. P. Lin, and M. H. Acuña (2001), Hot diamagnetic cavities upstream of the Martian bow shock, *Geophys. Res. Lett.*, *28*(5), 887–890, doi:10.1029/2000GL012289.

Joy, S. P., M. G. Kivelson, R. J. Walker, K. K. Khurana, C. T. Russell, and T. Ogino (2002), Probabilistic models of the Jovian magnetopause and bow shock locations, *J. Geophys. Res.*, *107*(A10), 1309, SMP 17–1–SMP 17–17, doi:10.1029/2001JA009146.

Köhnlein, W. (1996), Radial dependence of solar wind parameters in the ecliptic, *Sol. Phys.*, *169*(1), 209–213, doi:10.1007/BF00153841.

Masters, A., et al. (2009), Hot flow anomalies at Saturn's bow shock, *J. Geophys. Res.*, *114*, a08217, doi:10.1029/2009JA014112.

McComas, D. J., et al. (2013), The Jovian Auroral Distributions Experiment (JADE) on the Juno mission to Jupiter, *Space Sci. Rev.*, 1–97, doi:10.1007/s11214-013-9990-9.

McComas, D. J., et al. (2017), Plasma environment at the dawn flank of Jupiter's magnetosphere: Juno arrives at Jupiter, *Geophys. Res. Lett.*, *44*, 4432–4438, doi:10.1002/2017GL072831.

Paschmann, G., and P. W. Daly (Eds.) (2000), *Analysis Methods for Multi-Spacecraft Data*, *SR-001*, chap. 6, pp. 125–158, ESA Publ. Div., Noordwijk, Netherlands, electronic Edition.

Schwartz, S. (1995), Hot flow anomalies near the Earth's bow shock, *Adv. Space Res.*, *15*(8–9), 107–116, doi:10.1016/0273-1177(94)00092-F, proceedings of the D2.1 Symposium of {COSPAR} Scientific Commission D.

Schwartz, S. J., G. Paschmann, N. Sckopke, T. M. Bauer, M. Dunlop, A. N. Fazakerley, and M. F. Thomsen (2000), Conditions for the formation of hot flow anomalies at Earth's bow shock, *J. Geophys. Res.*, *105*(A6), 12,639–12,650, doi:10.1029/1999JA000320.

Schwartz, S. J., et al. (1985), An active current sheet in the solar wind, *Nature*, *318*, 269–271, doi:10.1038/318269a0.

Thomas, V. A., D. Winske, M. F. Thomsen, and T. G. Onsager (1991), Hybrid simulation of the formation of a hot flow anomaly, *J. Geophys. Res.*, *96*(A7), 11,625–11,632, doi:10.1029/91JA01092.

Thomsen, M. F., J. T. Gosling, S. A. Fuselier, S. J. Bame, and C. T. Russell (1986), Hot, diamagnetic cavities upstream from the Earth's bow shock, *J. Geophys. Res.*, *91*(A3), 2961–2973, doi:10.1029/JA091iA03p02961.

Thomsen, M. F., J. T. Gosling, S. J. Bame, K. B. Quest, C. T. Russell, and S. A. Fuselier (1988), On the origin of hot diamagnetic cavities near the Earth's bow shock, *J. Geophys. Res.*, *93*(A10), 11,311–11,325, doi:10.1029/JA093iA10p11311.

Uritsky, V. M., J. A. Slavin, G. V. Khazanov, E. F. Donovan, S. A. Boardsen, B. J. Anderson, and H. Korth (2011), Kinetic-scale magnetic turbulence and finite Larmor radius effects at mercury, *J. Geophys. Res.*, *116*, a09236, doi:10.1029/2011JA016744.

Uritsky, V. M., et al. (2014), Active current sheets and candidate hot flow anomalies upstream of Mercury's bow shock, *J. Geophys. Res. Space Physics*, *119*, 853–876, doi:10.1002/2013JA019052.